

MASSACHUSETTS INSTITUTE OF TECHNOLOGY
LINCOLN LABORATORY

MONOSTATIC AND BISTATIC SCATTERING
FROM THIN TURBULENT LAYERS IN THE ATMOSPHERE

R. K. CRANE

Group 61

TECHNICAL NOTE 1968-34

18 SEPTEMBER 1968

LEXINGTON

MASSACHUSETTS

· ERRATA SHEET

for

TECHNICAL NOTE 1968-34

The author has detected an error in Technical Note 1968-34
(R. K. Crane, "Monostatic and Bistatic Scattering from Thin
Turbulent Layers in the Atmosphere [U], " 18 September 1968).
Kindly insert this page into your copy of that report....

Page 1 Replace first equation by

$$\beta_{\perp}(\vartheta) = 8\pi^2 k^4 \tilde{\Phi}_n(\tilde{k} - k\hat{m}) \quad .$$

12 December 1968

Publications
M. I. T., Lincoln Laboratory
P. O. Box 73
Lexington, Massachusetts 02173

Monostatic and Bistatic Scattering from Thin Turbulent
Layers in the Atmosphere

ABSTRACT

Measurements were made of the scattering properties of thin turbulent layers at and above the tropopause. The Millstone Hill L-band radar was used to measure the backscatter cross section per unit volume of these layers as a function of time and space. An X-band forward scatter link was set up between Wallops Island, Virginia and Westford, Massachusetts to observe scattering from these layers. Although the radar could not provide observations of the common volume of the forward scatter link, for days where no clouds were observed in the vicinity of the tropopause, the radar observations of layers near the tropopause showed horizontal uniformity of height and backscatter cross section, and the radiosonde data taken near the radar and near the common volume showed similar wind and temperature structure near the tropopause, the signal strength on the forward scatter link and its dependence on scattering angle behaved in accordance with the prediction of turbulent scattering theory using the radar data as an input.

The radar observations have shown that on each day measurements were made, layers were detected near and above the tropopause. Turbulent layers in the stratosphere have been detected at heights up to 22 km. These layers provide one of the mechanisms for weak, long-distance troposcatter propagation.

Accepted for the Air Force
Franklin C. Hudson
Chief, Lincoln Laboratory Office

Monostatic and Bistatic Scattering from Thin Turbulent Layers in the Atmosphere

One of the mechanisms proposed for long distance transhorizon propagation is scattering from atmospheric turbulence. The turbulent scattering model has long been with us. The usual application of this model to the transhorizon scattering problem has met with little success. The dependence of long term median propagation loss measurements on frequency and on scattering angle has not agreed with the predictions of the turbulent scattering model. Because meteorological data point to the existence of turbulent regions in the atmosphere and because of a requirement for a technique to predict transhorizon field strengths given the meteorological data, an investigation of scattering by atmospheric turbulence was performed.

Turbulent Scattering:- A basic reference to scattering by turbulence is the work by Tatarski.¹ In this work the bistatic scattering cross section per unit volume is related to the spatial power spectral density of the distribution of refractive index by

$$\beta_{\perp}(\vartheta) = 8\pi k^2 \tilde{\Phi}_n(\underline{k} - \underline{k}^{\wedge})$$

$$\beta_{\parallel}(\vartheta) = \beta_{\perp}(\vartheta) \cos^2 \vartheta$$

where $\beta_{\perp}(\vartheta)$ = bistatic scattering cross section per unit volume for polarization perpendicular to the plane of scattering.

$\beta_{||}(\vartheta)$ = bistatic scattering cross section per unit volume for polarization parallel to the plane of scattering.

ϑ = scattering angle.

$k = 2\pi/\lambda$ = wave number, λ = wavelength.

$\tilde{\mathbf{k}}$ = vector pointing in the direction of propagation with a magnitude equal to k .

$\hat{\mathbf{m}}$ = unit vector pointing from the scatterer to the receiver.

$\tilde{\Phi}_n$ = spatial power spectrum of refractive index inhomogeneities.

For turbulent refractive index fluctuations

$$\tilde{\Phi}_n(\mathbf{x}) = \tilde{\Phi}_n(2k \sin \frac{\vartheta}{2}) = 0.033 C_n^2 (2k \sin \frac{\vartheta}{2})^{-11/3}; .01 < \frac{2\pi}{x} < 100 \text{ m}$$

as given by the semi-empirical similarity theory of turbulence for the inertial subrange. The classical application of turbulence scattering theory to the troposcatter problem has been to assume that C_n^2 is constant over the entire common volume determined by the intersection of the two antenna patterns and in general is constant over all space or decreases exponentially with height. With these assumptions, the bistatic scattering cross section per unit volume can be extracted from measured data and its frequency and angular dependence ascertained through the parameter x . Figure 1 shows the dependence of the turbulent scattering cross section upon the scale size $\ell = 2\pi/x$ and wavelength for three values of the scattering angle (referred to as troposcatter wavelength where the scattering angle is determined by the geometry

of the troposcatter link). In this figure are shown three turbulent scattering laws each for a different region of l . The scale sizes that mark the extent of a region are not as well defined as shown in the figure and the width of the different regions depends upon the mean properties of the medium. Figure 1 shows that to apply turbulent scatter theory for the inertial subrange, both the frequency and geometry have to be properly selected.

A second problem in the comparison of a turbulent scattering theory with measurements arises from the size of the turbulent region. Radar backscatter measurements and aircraft measurements show that the turbulent scattering volumes typically occur as thin horizontally stratified layers or patches. These layers are often only a few tens of meters thick and tens of kilometers across. An example of a radar observation of a thin layer is shown in Fig. 2. From atmospheric model computations based upon the methods of Vasil'chenko² that attempt to relate the C_n^2 value to the mean gradients of temperature, humidity, wind speed and wind shear, it has been shown that the relative magnitude of C_n^2 is a couple of orders of magnitude higher in the layer than in the region above or below the layer. This implies that a common volume averaged bistatic scattering cross section per unit volume can give misleading results in an attempt to compare measured cross sections with theory. It also implies that model computations of transhorizon field strengths using a turbulent scattering model should use a volume common only to the layer and the antenna patterns. Finally, since the scattering layer

is thin, the layer may act as a partially reflecting surface for vertical scale sizes larger than several tens of meters (frequencies below about 600 MHz on a 190 km scatter link).

Measurement Program:- A scattering model based upon turbulent scattering theory and the existence of isolated thin turbulent layers or patches can explain away many of the objections to the use of turbulent volume scattering as a transhorizon scattering mechanism. The questions then arise as to the occurrence of these thin scattering layers and a demonstration of transhorizon scattering as caused by these layers. To investigate both of these questions a measurement program was initiated at M. I. T. Lincoln Laboratory to detect high altitude layers with a radar and correlate their existence with the results of long distance troposcatter measurements. The measurement program used both the Millstone Hill L-band radar and an X-band troposcatter link operated from Wallops Island, Virginia to the Westford Communications Terminal. The common volume of the bistatic scattering system was not close enough to the radar to provide a direct measurement of the layered structure in the common volume. The structure within the volume was inferred, however, from the radar data, radiosonde soundings, and the angular dependence of the bistatic scattering data.

The characteristics of the L-band radar when used for weather studies are mentioned elsewhere.³ The radar system has a narrow bandwidth (0.6°), a relatively large pulse length (5 or 10 μ sec), and is capable of detecting

turbulent volumes large compared with the resolution volume with C_n^2 values higher than $10^{-16} \text{ m}^{-2/3}$ ($5 \times 10^{-18} \text{ cm}^{-2/3}$) at distances of 100 km. The radar wavelength is 0.23 meters and for turbulence measurements, it selects a scale size in the inertial subrange as shown in Fig. 1.

High altitude turbulent scattering as measured by the radar is generally weak and noise-like. The detection of turbulent scattering therefore consists of recognizing a spatial pattern of noise-like returns embedded in the receiver noise when displayed on a range, height display. Figure 2 shows such a display. The horizontal lines are the thin turbulent layers, the constant range targets are from ground clutter, and the curved lines are aircraft targets detected through the side lobes of the antenna pattern. The C_n^2 value for this layer is obtained from post-test analysis of 50 pulse incoherently averaged received signal values that are digitized and recorded on magnetic tape. For this particular layer $C_n^2 = 5 \times 10^{-16} \text{ m}^{-2/3}$ at a point 10 km high and 85 km in range. The true value may be higher if the layer is thinner than the resolution volume of the radar.

The X-band scatter link consisted of a transmitter located at the JAFNA radar facility on Wallops Island and a receiver at the Westford Communications Terminal as shown in Fig. 3. The transmitter facility consisted of a 1 kw cw source operated at 7.74 GHz and a 6-foot linearly polarized antenna. The receiver facility consisted of a 60-foot circularly polarized antenna, a cooled parametric rf amplifier, and a narrow band (500 cycle) phase lock tracking

receiver. The minimum detectable signal with this system was -160 dbm and corresponds to a troposcatter path loss of 148 db relative to free space.

The great circle path scatter link geometry is shown in Fig. 4. The path covered a great circle arc length of 628 km and, for an effective four-third earth radius atmospheric refraction model, the height to the lower edge of the common volumes was 5.5 km. The path was selected so only the regions of the atmosphere above 6 km were illuminated under normal propagation conditions. This was done because previous radar measurements had shown that typically one to three isolated scattering layers would be present above this height and, in order to measure the weak signal scattered by these layers, the stronger lower level layers should not be simultaneously visible to both the transmitter and receiver. If the lower, stronger layers were visible, the signals scattered from these layers could mask those of interest even if the strong layers were in the side lobe patterns of both antennas.

The forward scatter measurements were conducted by fixing the transmitter antenna pointing direction at a 0.8° elevation angle and along the great circle azimuth. The receiving antenna was scanned in azimuth and elevation so as to include the region of the layer illuminated by the transmitter. The geometry and frequency for the scatter experiment were chosen so the turbulent scattering process is described by the above equation valid in the inertial subrange. For model computations, both a C_n^2 value and a layer thickness must be chosen. Figure 5 shows that results of model computations for layers

at three heights and for elevation scans of the receiving antenna along the great circle direction. Although the scattering angle dependence of turbulence in the inertial subrange is included in the model calculations, the shape of the curve depends primarily on the transmitter antenna pattern and the thin layered geometry of the scattering volume. Other volume scatterers such as the ice crystals of a cirrus cloud will give curve shapes close to these because the scattering angle changes only slightly. From measurements corresponding to the model computations illustrated in Fig. 5 only the layer height may be determined. A value of C_n^2 times the layer thickness may also be determined for the layer but positive identification of the layer as turbulent scattering in contrast to particulate scattering cannot be made from these elevation scans alone. Figure 5 was generated without including the attenuation due to gaseous absorption. For this frequency the attenuation is of the order of 3 db and is nearly constant for the range of layer heights and angles used.

Results of Measurements:— Forward scatter measurements were made on 19 days during the months of March through May. On two of these days, rain along the path provided excessive attenuation and signals were barely detectable. The signal levels for the remaining days ranged, on average, from -144 dbm to noise for the elevation and azimuth angles used. Signals in excess of -110 dbm were often observed due to aircraft in the common volume but these data values were discarded. Elevation scans were made on 14 of the days and on 13 of these identification of a primary scattering layer could be

made.

Sample data for the 13th and 14 of March are shown in Fig. 6. On the curves are superimposed the best fit layer model and the C_n^2 to which it corresponds. The C_n^2 values are for an assumed layer thickness of 100 m and may deviate from this value due to the actual layer thickness. Because the form of the received power vs. elevation angle curve changes significantly with layer height, a layer height may easily be assigned. For both days the layers are near 8 km in height and agree with the position of the tropopause as determined from radiosonde soundings made close to the center of the common volume (JFK station on Fig. 2).

A direct comparison of radar and forward scattering measurements is impossible because of the distance from the radar to the common volume. The radar data has shown however that the turbulent patches, when they occur, usually occur at the same height over periods of several hours and distances of hundreds of kilometers. The actual life history of a single turbulent patch may however be brief being of the order of magnitude of tens of minutes. Figures 7 and 8 show radar detected layers at heights of 4, 6, 10 and 12 km for 8 May 1968. The data shows that the layered regions exist over several hundred kilometers near the Millstone Radar. If we assume this layer structure extends another hundred kilometers into the common volume of the scatter system, a layer height of 10 km and with $C_n^2 \sim 4 \times 10^{-16}$ would be expected. The lower layer of those in the common volume is expected since, at

the lower elevation angles and for equal scatter cross sections, the lower layer produces a higher signal strength. The forward scatter measurements for the same time are given in Fig. 9 and clearly show that the primary scattering layer is at 10 km and is in agreement with our expectation from the radar data.

Conclusions:— A thin-layered volume scattering model is proposed as a mechanism for long distance troposcatter propagation at microwave frequencies. Using a turbulent scattering model, the expected elevation angle dependence of received signals scattered from single layers near the tropopause was computed. The forward scatter measurements on 13 of 14 days are consistent with the model. For days with radar data and on which radiosonde data show similar soundings both at the radar and at the common volume, the height of troposcatter detected layers agrees with the height of the radar detected layers. The C_n^2 value detected by both the radar and the scatter system are of the same order of magnitude when compared. The discrepancies between these estimates arise because of the thinness and patchiness of turbulent layers.

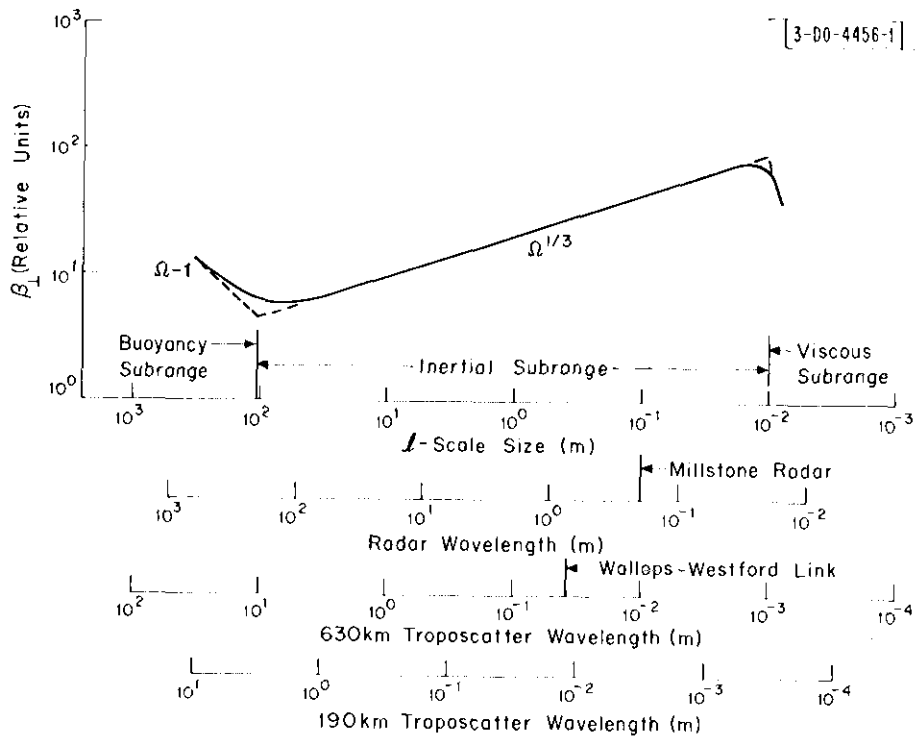
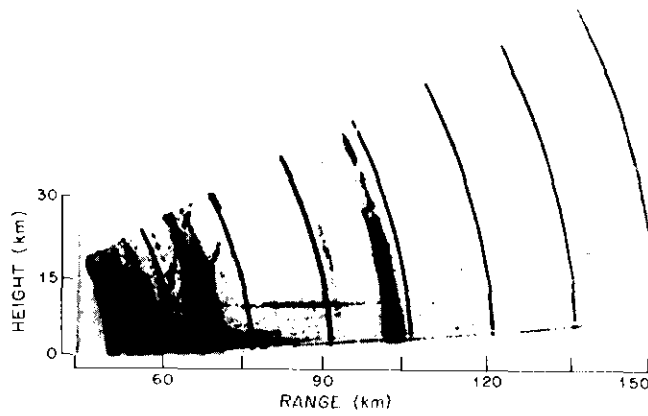


Fig. 1. Relative scattering cross section per unit volume vs. wavelength and scale.

[D0-4558-1]



9 FEB 1968 1410 GMT 70°AZIMUTH 0-30°ELEVATION
5- μ SEC PULSE 120 PRF 2.17-KW AVERAGE POWER

Fig. 2. Millstone Radar measurements.

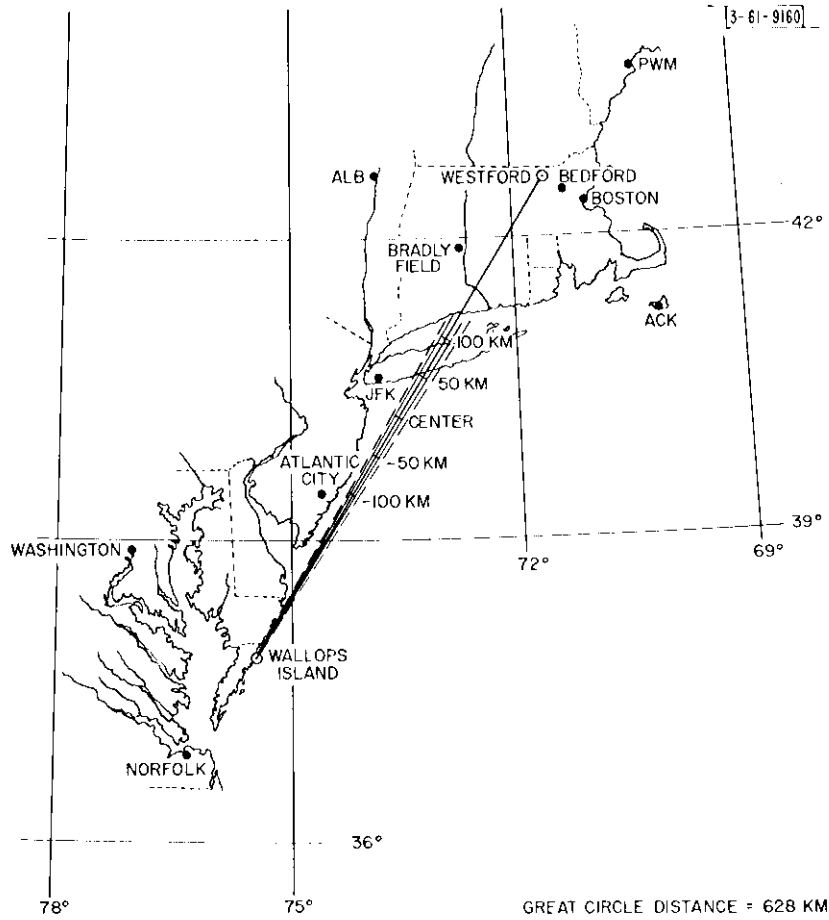


Fig. 3. Coastal map showing Wallops Island to Westford path.

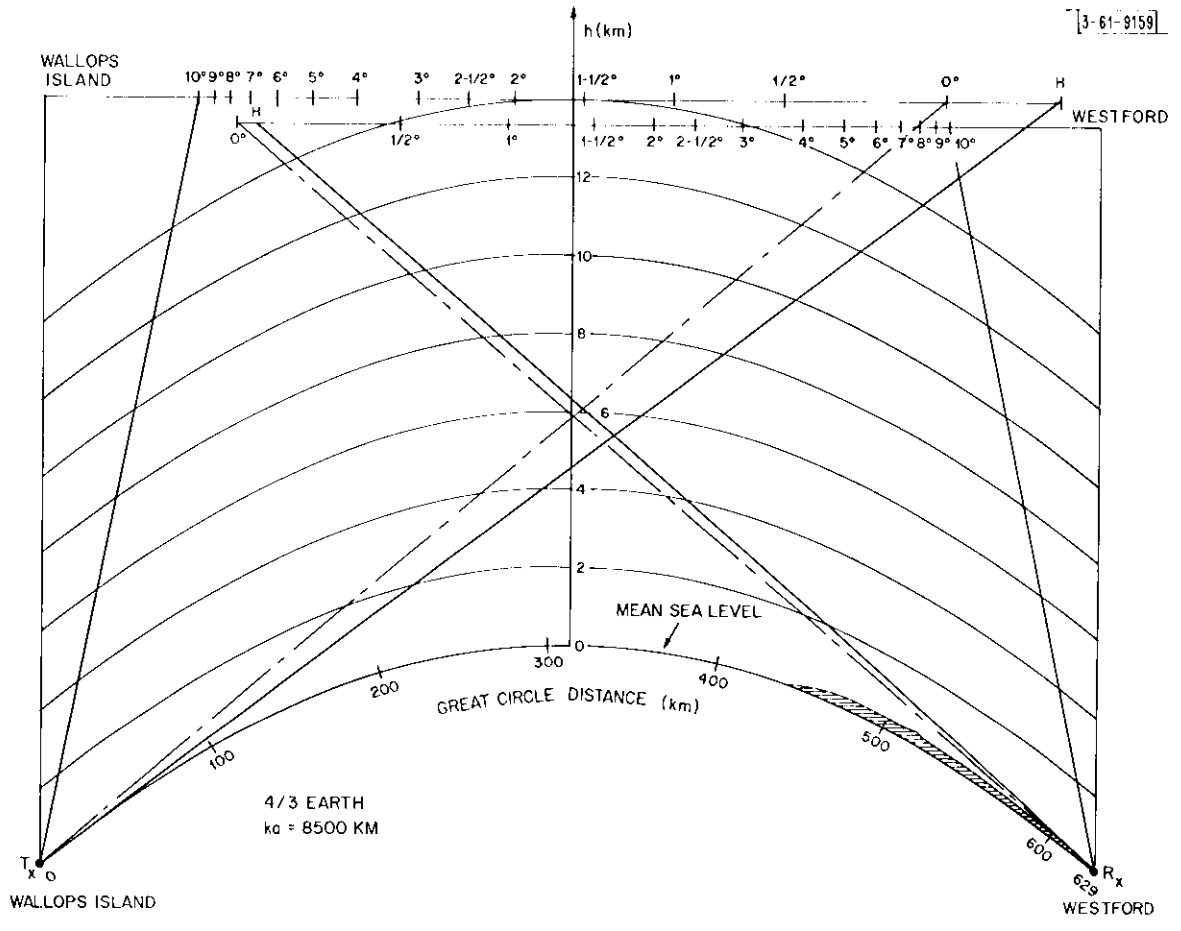


Fig. 4. Wallops Island - Westford cross section.

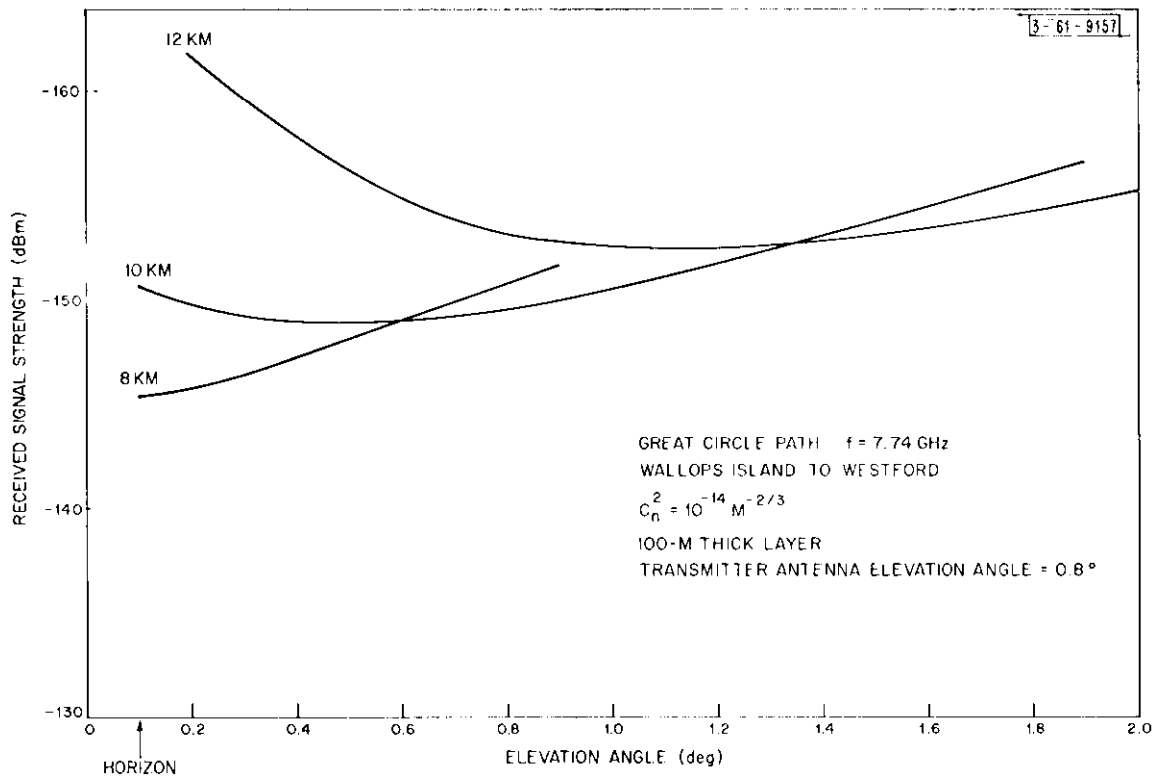


Fig. 5. Expected variation of received power with receiver antenna elevation angle.

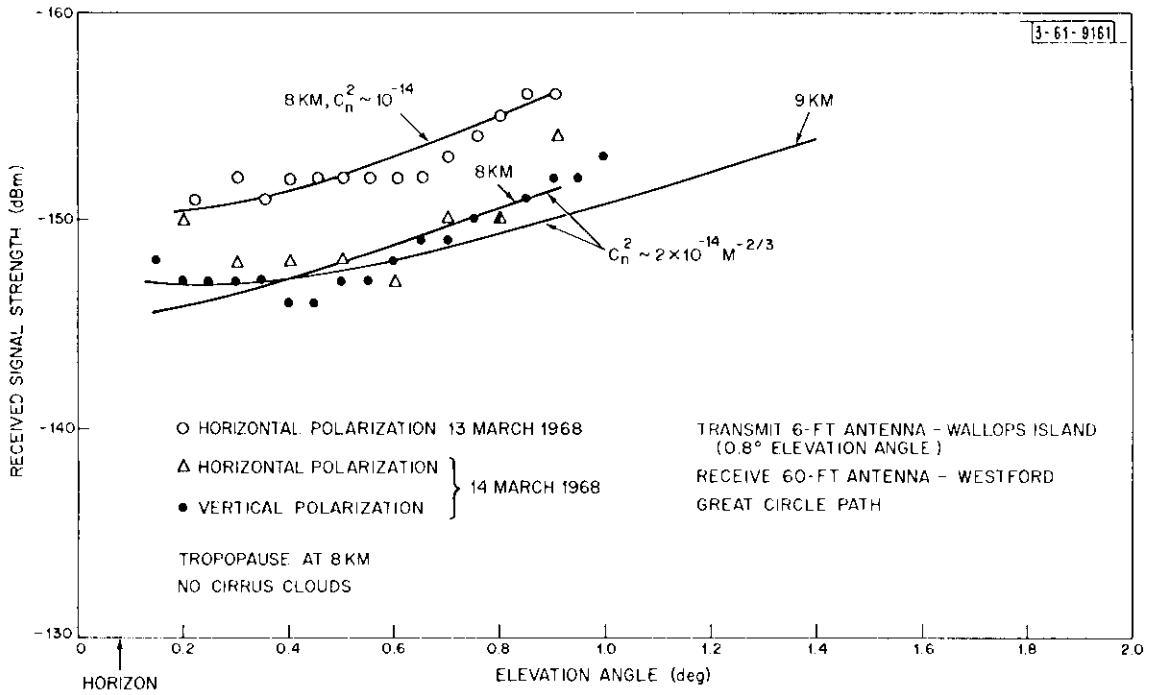


Fig. 6. Received signal vs. elevation angle of receiver antenna.

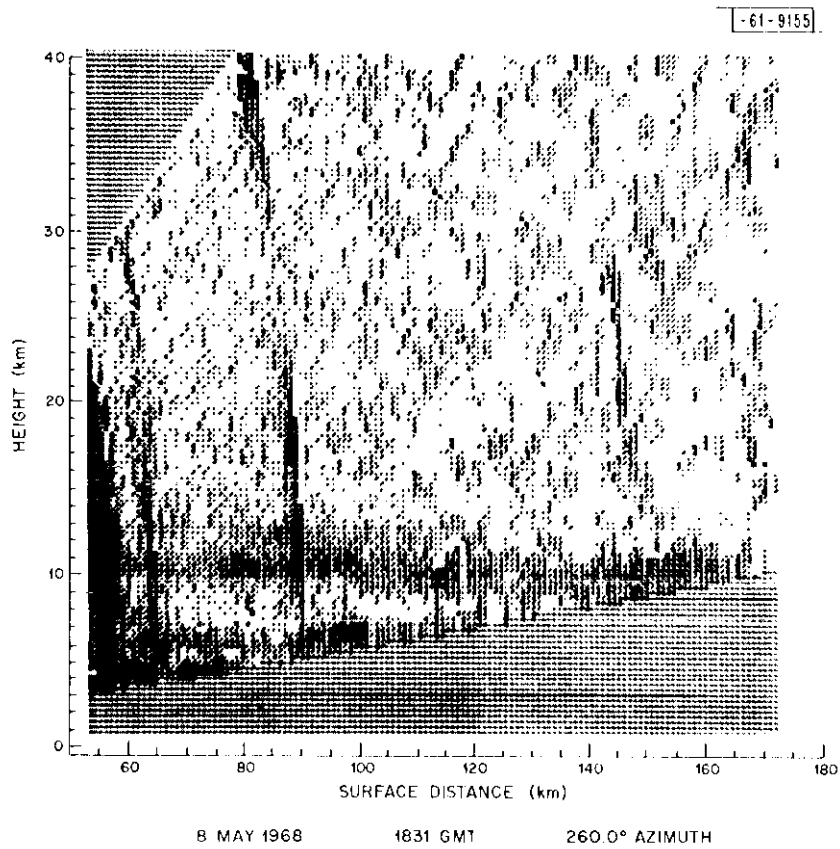


Fig. 7. Millstone Radar measurements - 8 May 1968.

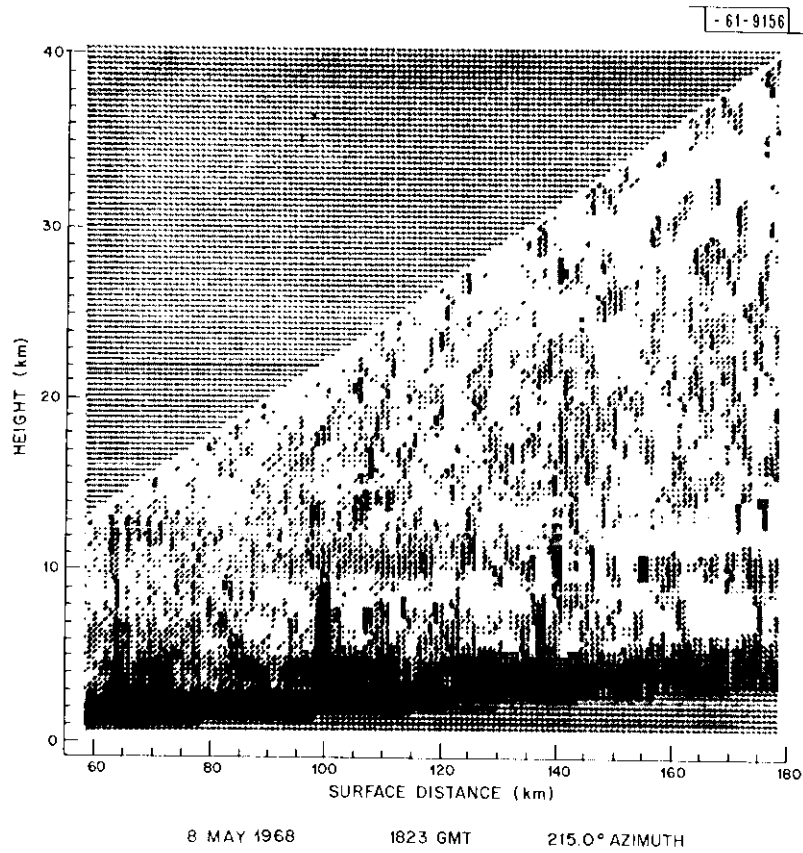


Fig. 8. Millstone Radar measurements - 8 May 1968.

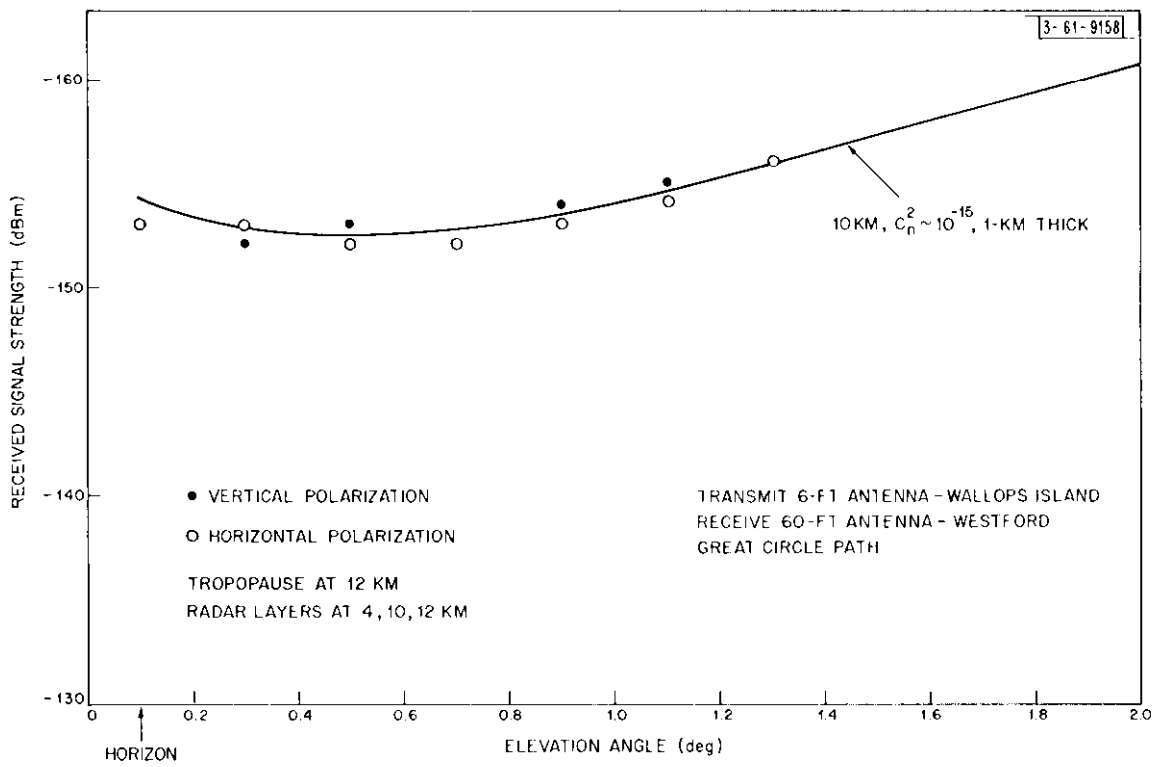


Fig. 9. Received signal strength vs. elevation angle of receiving antenna.

REFERENCES

1. V. I. Tatarski, Wave Propagation in a Turbulent Medium, McGraw-Hill Book Company, New York (1961).
2. V. I. Vasil'chenko, "Relationship Between the Turbulence Coefficient and the Vertical Distribution of Temperature and Winds in the Lower 300-Layer as indicated by Ballon Data," *Trudy Glavnoy Geofizicheskoy Observatorii*, No. 185, 68-71 (1966).
3. R. K. Crane, "Simultaneous Radar and Radiometer Measurements of Rain Shower Structure," (to be published).

